Characterization of *htrB* and *msbB* Mutants of the Light Organ Symbiont *Vibrio fischeri*[▽]

Dawn M. Adin,[1] Nancy J. Phillips,[2] Bradford W. Gibson,[2] Michael A. Apicella,[3] Edward G. Ruby,[4] Margaret J. McFall-Ngai,[4] Daniel B. Hall,[5] and Eric V. Stabb[1]*

Departments of Microbiology[1] and Statistics,[5] University of Georgia, Athens, Georgia; Department of Pharmaceutical Chemistry, University of California, San Francisco, California[2]; Department of Microbiology, University of Iowa College of Medicine, Iowa City, Iowa 52242[3]; and Department of Medical Microbiology and Immunology, University of Wisconsin, Madison, Wisconsin[4]

Bacterial lipid A is an important mediator of bacterium-host interactions, and secondary acylations added by HtrB and MsbB can be critical for colonization and virulence in pathogenic infections. In contrast, *Vibrio fischeri* lipid A stimulates normal developmental processes in this bacterium's mutualistic host, *Euprymna scolopes*, although the importance of lipid A structure in this symbiosis is unknown. To further examine *V. fischeri* lipid A and its symbiotic function, we identified two paralogs of *htrB* (designated *htrB1* and *htrB2*) and an *msbB* gene in *V. fischeri* ES114 and demonstrated that these genes encode lipid A secondary acyltransferases. *htrB2* and *msbB* are found on the *Vibrio* "housekeeping" chromosome 1 and are conserved in other *Vibrio* species. Mutations in *htrB2* and *msbB* did not impair symbiotic colonization but resulted in phenotypic alterations in culture, including reduced motility and increased luminescence. These mutations also affected sensitivity to sodium dodecyl sulfate, kanamycin, and polymyxin, consistent with changes in membrane permeability. Conversely, *htrB1* is located on the smaller, more variable vibrio chromosome 2, and an *htrB1* mutant was wild-type-like in culture but appeared attenuated in initiating the symbiosis and was outcompeted 2.7-fold during colonization when mixed with the parent. These data suggest that *htrB2* and *msbB* play conserved general roles in vibrio biology, whereas *htrB1* plays a more symbiosis-specific role in *V. fischeri*.

Vibrio fischeri is a bioluminescent bacterium that forms a mutualistic symbiosis with *Euprymna scolopes*, the Hawaiian bobtail squid. *E. scolopes* supports the growth and bioluminescence of *V. fischeri* in a specialized light organ (40), and the bacterial luminescence is apparently used by the squid in a camouflaging behavior (23). *V. fischeri* is more abundant in *E. scolopes* habitats, reinforcing the belief that the relationship is beneficial for both partners (28). Among the hundreds of bacterial species present in Hawaiian waters, only *V. fischeri* is able to colonize the *E. scolopes* light organ. This specific colonization triggers developmental changes in light organ tissue, and it is clear that *E. scolopes* identifies and responds to signals from *V. fischeri* (32). Although the mechanisms underlying the specificity, signaling, and persistence of this symbiosis are not entirely clear, previous studies suggested that a key molecule in some of these symbiotic processes is *V. fischeri*'s lipopolysaccharide (LPS) (13).

LPS comprises 70% of the outer membrane of gram-negative bacteria and has the following three main components: (i) O antigen, which is a variable hydrophilic polysaccharide that projects into the environment; (ii) a relatively conserved central core of sugars; and (iii) lipid A, which anchors LPS into the outer membrane. The innate immune systems of many animals recognize lipid A through LPS-binding protein and Toll-like receptors (20, 21), which stimulate inflammation to attract more host immune cells to clear pathogenic infections (8, 33). Indeed, the strong, sometimes overreactive immune response to lipid A has earned LPS its alternate name "endotoxin." Interestingly, LPS-responsive elements of the innate immune system are conserved in *E. scolopes* (14), and *V. fischeri* LPS elicits host responses that typify normal development of this mutualistic symbiosis. For example, *V. fischeri* LPS or lipid A stimulates apoptosis in a specific field of ciliated cells on the light organ (13), and LPS acts synergistically with peptidoglycan to induce light organ morphogenesis (25).

Changes in lipid A structure, in particular the elimination or exchange of certain secondary acylations, affect the virulence of pathogens and the bioactivity of LPS. Accordingly, some pathogens regulate their lipid A structure and acylation patterns in adapting to a host environment (16, 39). Mutant analyses have been useful in unraveling the relationship between lipid A structure and function in such infections. For example, mutations in genes that encode secondary acyltransferases, such as *htrB* (*lpxL*) and *msbB* (*lpxM*), can affect lipid A structure, thereby altering lipid A bioactivity and pathogen virulence (10, 22, 43, 49, 52).

The relationship between lipid A structure and function in nonpathogenic animal-bacterium interactions remains largely unknown. Citing precedent in pathogenic interactions and experiments with foreign LPS, Foster et al. suggested a relationship between *V. fischeri* lipid A acylation patterns and bioactivity in its symbiosis with *E. scolopes* (13). Our goal in this study was to determine how secondary acylation of lipid A affects the biology of *V. fischeri*, particularly its symbiotic phenotypes. We identified three lipid A secondary acyltransferases

TABLE 1. Bacterial strains, plasmids, and oligonucleotides

Strain, plasmid, or oligonucleotide	Relevant characteristics or sequence[a]	Source or reference
Strains		
E. coli strains		
DH5α	F⁻ φ80d*lacZ*Δ (*lacZYA-argF*)*U169 deoR supE44 hsdR17 recA1 endA1 gyrA96 thi-1 relA1*	18
DH5α-λ*pir*	DH5α lysogenized with λ*pir*	11
MKV15	W3110 *lpxP::kan lpxM::Ωcam lpxL::*Tn*10*	56
TOP10	F⁻ *mcrA* Δ(*mrr-hsdRMS-mcrBC*) φ80*lacZ*ΔM15 Δ*lacX74 recA1 ara*Δ*139* Δ(*ara-leu*)*7697 galU galK rpsL* St^r *endA1 nupG*	Invitrogen
W3110	F⁻ *rph-1 IN*(*rrnD-rrnE*)*1* λ⁻	56
V. fischeri strains		
AO340	*htrB1::erm* allele from pEVS97 in DMA333 (*htrB1::erm* Δ*htrB2* Δ*msbB*)	This study
DMA310	Δ*htrB2::erm* allele from pDMA24 in ES114 (Δ*htrB2::erm*)	This study
DMA311	Δ*htrB2* allele from pDMA22 in DMA310 (Δ*htrB2*)	This study
DMA321	Δ*msbB* allele from pHKG2 in HG320 (Δ*msbB*)	This study
DMA330	*htrB1::erm* allele from pEVS97 in DMA311 (Δ*htrB1::erm* Δ*htrB2*)	This study
DMA331	*htrB1::erm* allele from pEVS97 in DMA321 (Δ*htrB1::erm* Δ*msbB*)	This study
DMA332	Δ*msbB::erm* allele from pHKG4 in DMA311 (Δ*msbB::erm* Δ*htrB2*)	This study
DMA333	Δ*msbB* allele from pHKG2 in DMA332 (Δ*htrB2* Δ*msbB*)	This study
ES114	Wild-type *E. scolopes* isolate	1
EVS300	*htrB1::erm* allele from pEVS97 in ES114 (*htrB1::erm*)	This study
HG320	Δ*msbB::erm* allele from pHKG4 in ES114 (Δ*msbB::erm*)	This study
Plasmids		
pCR-BluntII-TOPO	Topo PCR cloning vector; Kn^r	Invitrogen
pDMA5	*oriV*$_{p15A}$ *oriT*$_{RP4}$ *lacZ*α Cm^r	11
pDMA7	*htrB1* (1.4 kb) BglII-digested PCR product (primers dma19 and dma20, ES114 template) in BamHI-digested pDMA5	This study
pDMA8	*msbB* (1.5 kb) PCR product (primers dma7 and dma8, ES114 template) in pCR-BluntII-TOPO	This study
pDMA9	pDMA8 SpeI/XhoI *msbB* fragment in SpeI/XhoI-digested pDMA5	This study
pDMA10	*htrB2* (3.8 kb) PCR product (primers dma15 and dma16, ES114 template) in pCR-BluntII-TOPO	This study
pDMA11	*htrB2* (1.5 kb) PCR product (primers dma13 and dma14, ES114 template) in pCR-BluntII-TOPO	This study
pDMA12	*htrB1* (3.8 kb) PCR product (primers dma3 and dma4, ES114 template) in pCR-BluntII-TOPO	This study
pDMA13	*msbB* (4.0 kb) PCR product (primers dma9 and dma10, ES114 template) in pCR-BluntII-TOPO	This study
pDMA15	pDMA12 BamHI/ApaI *htrB1* fragment in BglII/ApaI-digested pEVS118	This study
pDMA19	*htrB1* in-frame deletion; PCR product (primers dma5 and dma6, pDMA15 template) was BglII digested and self-ligated	This study
pDMA20	pDMA10 BamHI/EcoRV *htrB2* fragment in BglII/AscI-digested and Klenow-filled pEVS118	This study
pDMA22	*htrB2* in-frame deletion; PCR product (primers dma17 and dma18, pDMA20 template) was BglII digested and self-ligated	This study
pDMA23	pDMA11 SpeI/XhoI *htrB2* fragment in SpeI/XhoI-digested pDMA5	This study
pDMA24	pEVS122 BamHI/BglII Em^r fragment in pDMA22 BglII site	This study
pDMA25	pJLB2 EcoRV/SpeI *dfr*1 fragment, Klenow filled, in pDMA7 EcoRV site	This study
pDMA27	pJLB2 EcoRV/SpeI *dfr*1 fragment, Klenow filled, in pDMA23 EcoRV site	This study
pDMA28	pJLB2 EcoRV/SpeI *dfr*1 fragment, Klenow filled, in pDMA5 EcoRV site	This study
pDMA34	pDMA7 HincII/SpeI *htrB1* fragment in HincII/SpeI-digested pVSV105	This study
pDMA42	pDMA8 SpeI/XbaI *msbB* fragment in XbaI-digested pVSV105	This study
pDMA43	pDMA11 SpeI/XbaI *htrB2* fragment in XbaI-digested pVSV105	This study
pDMA114	pJLB2 EcoRI *dfr*1 fragment, Klenow filled, in EcoRV-digested pDMA8	This study
pDFR1	*Vibrio salmonicida dfr*1 (GenBank accession no. AJ277063) in pUC19; Ap^r Tp^r	H. Sørum
pEVS79	*oriV*$_{ColE1}$ *oriT*$_{RP4}$ Cm^r	47
pEVS94	*oriV*$_{R6Kγ}$ *oriT*$_{RP4}$ Em^r	47
pEVS96	*oriV*$_{ColE1}$ *oriT*$_{RP4}$ Cm^r; EcoRI-HindIII *htrB1* fragment from ES114 in pEVS79	This study
pEVS97	pEVS94 EcoRV Em^r fragment in BsaBI site in *htrB1* on pEVS96	This study
pEVS104	*oriV*$_{R6Kγ}$ *oriT*$_{RP4}$ Kn^r; RP4-derived conjugal helper plasmid	47
pEVS118	*oriV*$_{R6Kγ}$ *oriT*$_{RP4}$ Cm^r	11
pEVS122	*oriV*$_{R6Kγ}$ *oriT*$_{RP4}$ *lacZ*α Em^r	11
pHKG1	pDMA13 BamHI/ApaI *msbB* fragment in BglII/ApaI-digested pEVS118	This study

TABLE 1—*Continued*

Strain, plasmid, or oligonucleotide	Relevant characteristics or sequence[a]	Source or reference
pHKG2	*msbB* in-frame deletion; PCR product (primers dma11 and dma12, pHKG1 template) was StuI digested and self-ligated	This study
pHKG4	pEVS122 EcoRV Em[r] fragment in StuI-digested pHKG2	This study
pJLB2	*dfr1* PCR product (primers JB1 and JB2, pDFR1 template) in pCR-BluntII-TOPO; Kn[r] Tp[r]	This study
pVSV103	*oriT*$_{RP4}$ *oriV*$_{pES213}$ Kn[r] *lacZ*	12
pVSV105	*oriV*$_{R6K\gamma}$ *oriT*$_{RP4}$ *oriV*$_{pES213}$ Cm[r] *lacZ*α	12
Oligonucleotides		
dma3	TACCCAAGGCTTAATGAGCCGCCCC	This study
dma4	CGCCTAAACGCTTTGAAGCTTACGGCTGGC	This study
dma5	CGGAGATCTCATCAAAACTAAGACACC	This study
dma6	GGCAGATCTTAACAATTCTTTTGCCGTG	This study
dma7	GGCTTAGTGTTAGTAAGTAAAAGGCAG	This study
dma8	CCCGCAGAACTGTGTAATTCTACGGG	This study
dma9	GGTAATTTTTGCGGAGAGTATCAGTTCG	This study
dma10	CCTAAAGCTTGAGCAATAAACGTTGCGCC	This study
dma11	GCCAGGCCTCATGAATTGCTTCACTGTCTCATTATTATAAG	This study
dma12	GGCAGGCCTTAACTTTTTTGTTATTCGGCTCTTATTTGAAACC	This study
dma13	GCGTTATATCGCCATTTCCCAAGC	This study
dma14	GCGATCACCAAGGCTAGCCGCCC	This study
dma15	GCGGTCTAGAGCGGGCCCCAACTCGTGAAGCC	This study
dma16	CGCCTCTAGAGCGTAATGCCATAATGATTGGCG	This study
dma17	GCGGAGATCTCATCGTGAGCCTATTTTATCTAATTAATTATTGG	This study
dma18	GCGGAGATCTTAGGGCGTGTCAGGATAAATAATGAAAACC	This study
dma19	GGCAGATCTCAGATGGTTTGATTAATATTGAATCAGG	This study
dma20	CGGAGATCTCGTAGGTTTCGGTGGCAAGATCATCGGC	This study
EVS69	GAAACTGGTATTACTTGGTTTTGG	This study
EVS72	TACTGCAAAAAAAGGAACAAAAAC	This study
JB1	GCGCTTCGAACTCTGAGGAAGAATTGTG	11
JB2	GCGCCCTAGGTTAGTTAGTTAACCCTTTTGCCAGA	11

[a] Ap[r], ampicillin resistance; Cm[r], chloramphenicol resistance; Em[r], erythromycin resistance; Kn[r], kanamycin resistance; Tp[r], trimethoprim resistance; St[r], streptomycin resistance. Oligonucleotide sequences are given 5′ to 3′.

in *V. fischeri*, mutated the respective genes singly and in combination, and characterized the mutants in culture and in the host. Some of these mutants had deleterious phenotypes in culture; however, one mutant displayed a symbiosis-specific defect.

MATERIALS AND METHODS

Bacterial strains and culture conditions. The strains used in this study are listed in Table 1. When added to LB medium (31) or a supplemented phosphate-buffered minimal Kozak medium (56) for selection of *Escherichia coli*, chloramphenicol (Cm), kanamycin (Kn), and trimethoprim (Tp) were used at concentrations of 20, 40, and 10 μg ml^{-1}, respectively. For selection of *E. coli* with erythromycin (Em), 150 μg ml^{-1} was added to brain heart infusion medium (Difco, Sparks, MD). Unless otherwise noted, *E. coli* was incubated at 37°C, except for strain MKV15 (56), which was incubated at 28°C. *V. fischeri* was grown in LBS medium (45) or SWT medium (1) made with Instant Ocean (Aquarium Systems, Mentor, OH). When added for selection of *V. fischeri*, Cm, Kn, Em, and Tp were used at concentrations of 2, 100, 5, and 10 μg ml^{-1}, respectively. *V. fischeri* was grown at 28°C or 24°C. Agar was added to a final concentration of 1.5% for solid media.

Molecular genetics. Plasmids (Table 1) were generated using standard cloning methods and were isolated using a QIAprep spin miniprep kit (Qiagen, Valencia, CA). Restriction and modification enzymes were obtained from New England Biolabs (Beverly, MA). A Zero Blunt TOPO PCR cloning kit (Invitrogen, Carlsbad, CA) was used to clone PCR products into pCR-BluntII-TOPO. DNA fragments were purified using either a Wizard DNA cleanup kit (Promega Corp., Madison, WI) or a DNA Clean & Concentrator 5 kit (Zymo Research, Orange, CA). PCR was performed using an iCycler (Bio-Rad Laboratories, Hercules, CA), with *Pfu*-Turbo (Stratagene, La Jolla, CA) to amplify *dfr1* or with KOD HiFi DNA polymerase (Novagen, Madison, WI) for other PCR-based cloning.

DNA sequencing was conducted on an ABI automated DNA sequencer at the University of Georgia Integrated Biotech Laboratories, and oligonucleotides were obtained from either the University of Georgia Integrated Biotech Laboratories or Integrated DNA Technologies (Coralville, IA).

Mutant alleles were generated as delineated in Table 1. In most instances, the target gene was amplified from *V. fischeri* ES114, with ~1.5 kb of flanking DNA on either side, using the genome sequence to guide primer design. PCR products were cloned into pCR-BluntII-TOPO and subcloned into the mobilizable suicide plasmid pEVS118. A second round of PCR outward from the target gene amplified sequences flanking the target as well as the vector. BglII (or StuI) sites were placed on the ends of the primers for the secondary PCR, and the PCR amplicon was digested with BglII (or StuI) and self-ligated to generate a deletion target (Δtarget) allele. These constructs were sequenced to ensure that no unintended changes were incorporated. An Em resistance (*erm*) cassette was inserted into the BglII (or StuI) site to generate Δtarget::*erm* alleles, each plasmid was transferred into *V. fischeri* ES114 by triparental mating (47), and single and double recombinants were selected and screened as previously described (45). The Δtarget::*erm* alleles were exchanged onto the chromosome first and then replaced by unmarked Δtarget alleles, using Em sensitivity as a screen. Exchange of each mutation onto the genome was confirmed by PCR analysis. In the lone exception to this approach, the *htrB1* gene was cloned before the *V. fischeri* genome was sequenced by using PCR amplification with primers EVS69 and EVS72, which target conserved *htrB* sequences, to identify an *htrB1*-containing clone in increasingly smaller clone pools of an ES114 genomic library (55). Subsequent subcloning resulted in pEVS97, which contains *htrB1* centered on a 4.2-kb fragment of ES114 DNA and interrupted by insertion of *erm* at a unique BsaBI site.

Plasmids for complementation were generated by amplifying each gene with ~500 bp of upstream sequence and cloning the fragments first into pCR-BluntII-TOPO and then into pVSV105 for complementation of *V. fischeri* mutants. Each gene was also subcloned into pDMA5, and a Tp resistance cassette was added to allow selection in MKV15.

LPS and lipid A purification and analysis. LPS was purified from *E. coli* or *V. fischeri* strains as described previously (38). Lipid A from *E. coli* W3110, MKV15, or MKV15 carrying a plasmid with *V. fischeri htrB1*, *htrB2*, *msbB*, or no insert was obtained from the LPS by mild acid hydrolysis (1% acetic acid, 2 h, 100°C) followed by centrifugation and washing (36). Lipid A pellets were partitioned in CHCl$_3$-methanol (MeOH)-H$_2$O (10:5:6), and the bottom organic layers plus interfaces were saved and evaporated to dryness under a stream of N$_2$.

Lipid A samples were analyzed by matrix-assisted laser desorption ionization–time-of-flight mass spectrometry (MALDI-TOF MS) on a Voyager DESTR Plus instrument (Applied Biosystems, Framingham, MA) equipped with a 337-nm nitrogen laser. All samples were run in the negative-ion linear or reflectron mode with delayed extraction and a 20-kV extraction voltage. Prior to analysis, lipid A samples were dissolved in CHCl$_3$-MeOH (3:1) and desalted with cation-exchange resin (Dowex 50W-X8, NH$_4^+$ form; Bio-Rad, Hercules, CA). Samples were then mixed with an equal volume of matrix solution, i.e., saturated 6-chloro-2-mercapto-benzothiazole in CHCl$_3$-MeOH (3:1), spotted onto a stainless steel target, and air dried. Approximately 200 laser shots were acquired for each sample, and the spectra were baseline corrected and smoothed with a five-point Gaussian function. Spectra were calibrated externally with angiotensin II, renin substrate tetradecapeptide, and insulin chain B (oxidized) (all from Sigma, St. Louis, MO). Ions measured by reflectron MALDI-TOF are reported as monoisotopic masses of the ^{12}C-containing component.

GC-MS analysis of fatty acids derived from lipid A. Approximately 100 μg of *E. coli* or *V. fischeri* lipid A sample was treated with 0.5 ml of 10% (wt/wt) BF$_3$-methanol (Supelco, Inc., Bellefonte, PA) and heated at 100°C for 6 h. After cooling to room temperature, the samples were partitioned between saturated NaCl and high-performance liquid chromatography-grade hexanes (Aldrich, St. Louis, MO), extracted, and evaporated to dryness under a stream of N$_2$ (36). The fatty acid methyl esters (FAMEs) were redissolved in hexanes and analyzed by gas chromatography-MS (GC-MS) in the electron impact mode, using a Varian Saturn 2100T ion-trap MS/MS interfaced with a Varian 3900 GC (Varian, Inc., Walnut Creek, CA). Injections were made with a 1:20 or a 1:50 split, with the injector temperature set at 200°C and the ion-trap temperature set at 195°C. FAMEs were separated on a 30-m by 0.25-mm BPX70 column with a 0.25-μm film thickness (SGE, Inc., Austin, TX), using helium as the carrier gas (constant column flow, 1.0 ml/min). The initial oven temperature was 90°C for 3.5 min, followed by a temperature gradient from 90°C to 220°C at 4°C min^{-1}. A mixture of bacterial acid methyl esters (Matreya, LLC, Pleasant Gap, PA) was used as a GC-MS standard solution.

Antimicrobial assays. To assess growth inhibition by sodium dodecyl sulfate (SDS), polymyxin B, or Kn, the agent of interest was serially diluted in water in ≤2-fold steps, 100 μl of each dilution was added to 900 μl of SWT medium in a 10-mm test tube, 10 μl of mid-log-phase culture was added, cultures were grown at 24°C until the control tubes lacking the test substance reached an optical density at 595 nm (OD$_{595}$) of between 0.5 and 0.9, and then the OD$_{595}$ of the culture in each tube was determined. The inhibitory concentration yielding 50% of the OD$_{595}$ in the antimicrobial-free control (IC$_{50}$) was determined by plotting OD$_{595}$ values from three independent trials, each with three replicates/dilutions of the substrate, versus the log of the dose. The IC$_{50}$ was calculated using a model fitted to all nine trials with the nonlinear mixed-effect function in S-PLUS software (37).

To determine whether the IC$_{50}$ of each mutant was significantly different from that of the wild type, we utilized a three-parameter logistic model in which the IC$_{50}$ parameter (as well as the other two model parameters) was modeled with mixed effects, including fixed factorial and interaction effects of the three mutant alleles, to account for differences among the strains. F tests of standard analysis of variance (ANOVA) main effect and interaction hypotheses were used to test for allelic interactions leading to nonadditive effects on IC$_{50}$. In addition, 95% confidence intervals were generated for each strain's estimated IC$_{50}$, and F tests were performed for pairwise contrasts between each strain and the wild type.

Motility assays. Motility was assessed as described previously (9, 57). Cultures were grown to mid-log phase (OD$_{595}$, 0.5) at 24°C, 5 μl of the culture was spotted onto a quadrant of an SWT soft (0.25%) agar plate, and diameter measurements of the movement away from the point of inoculation were taken every hour. For each spot, a slope estimate was obtained from a simple linear regression of diameter over time to quantify the velocity of spread, or motility rate. The resulting six slopes per strain were then analyzed using one-way ANOVA to test for equal mean motility rates across strains, and Tukey's studentized range test was used to perform pairwise comparisons among the strains at a simultaneous significance level of alpha = 0.001. The ANOVA model was fit using weighted least squares, weighted by the precision (inverse estimated variance) of each slope estimate. All analyses were performed using the statistical program SAS (SAS Institute Inc., Cary, NC).
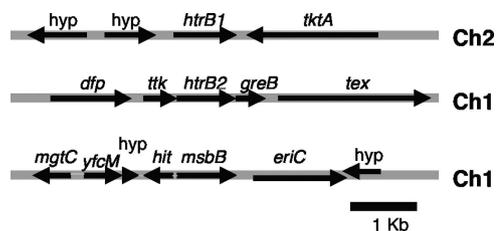

FIG. 1. Chromosomal location and orientation of *htrB1*, *htrB2*, and *msbB* in *V. fischeri* ES114. Open reading frames encoding hypothetical proteins are designated "hyp." Blast-P searches of the National Center for Biotechnology Information database were used to determine homologies (e < 10^{-15}) and to assign names for genes flanking *htrB1*, *htrB2*, and *msbB*. Arrows indicate gene orientations. Ch1 and Ch2 indicate localization to chromosomes 1 and 2, respectively.

Microscopy. One-hundred-microliter aliquots of mid-log-phase cultures were fixed in Parducz solution (3:3:1 4% OsO$_4$-2% saline-saturated HgCl$_2$) (35) for 1 h. Each sample was pelleted, washed twice with 2% saline, dehydrated with sequential washes of 25, 30, 50, 70, 85, 90, and 100% ethanol for 10 min each, and applied with a 5-ml syringe to a 13-mm-diameter, 0.2-mm Millipore filter. Samples were dried in a Samdri-780A critical point drying apparatus with liquid CO$_2$, coated with gold until they were approximately 76.5 Å thick by using a SPI-module sputter coater, and examined with a LEO 982 FE scanning electron microscope running at 5 kV.

Luminescence assays. Luminescence of cells cultured in SWT medium at 24°C was determined using a TD 20/20 luminometer (Turner Designs, Sunnyvale, CA). Symbiotic luminescence of individual animals was measured using an LS6500 scintillation counter (Beckman Coulter, CA).

Competition in mixed cultures. Mutants were competed against the wild type in mixed cultures with one of the strains marked by pVSV3, which expresses *lacZ*, allowing blue-white screening of strain ratios on LBS plates supplemented with 50 or 100 μg ml^{-1} 5-bromo-4-chloro-3-indolyl-β-D-galactoside (X-Gal). To ensure that plasmid loss or bias in blue-white scoring did not skew results, each mutant's competitiveness was calculated by averaging the results for mutant/pVSV3 mixed with ES114 (wild type) and mutant mixed with ES114/pVSV3. Individual strains were grown to mid-log phase and mixed ~1:1, and the culture was dilution plated to determine the starting strain ratio. The mixed culture was then subcultured 2^{10}-fold, regrown to the starting OD$_{595}$, and plated on LBS medium containing X-Gal to determine the strain ratio after 10 generations. The process of subculturing, regrowth, and plating was repeated for later generations. The relative competitiveness index (RCI) of each mutant was calculated by dividing the ratio of mutant to wild type by the starting ratio. An RCI of <1 indicates that the mutant strain was outcompeted, an RCI of >1 indicates that the wild-type strain was outcompeted, and an RCI of 1 indicates no competitive difference between strains.

Squid colonization assays. For infection with individual *V. fischeri* strains, *E. scolopes* juveniles were inoculated within 4 h of hatching as previously described (40). Briefly, between 9 and 30 hatchlings were placed in 100 ml of filter-sterilized seawater to which the strain of interest was added, left in this inoculum for 3 h, and then transferred to 5 ml of bacterium-free seawater in a 20-ml glass vial. After assay of luminescence (see above), squid were homogenized, and the homogenates were serially diluted and plated to determine the CFU per squid. To determine a mutant's competitiveness relative to ES114, juvenile squid were exposed to an ~1:1 mix of the strains for 14 h and then moved to bacterium-free water. After 48 h, the squid were homogenized and dilution plated to determine the ratio of mutant to wild type. The RCI was determined as described above by dividing the mutant to wild-type ratio in each individual squid by the ratio in the inoculum. The average RCI and statistical significance were calculated using log-transformed data.

RESULTS

Analysis of putative lipid A secondary acyltransferase genes in *V. fischeri*. To begin addressing the relationship between *V. fischeri* lipid A structure and its symbiotic function, we identified homologs of lipid A secondary acyltransferase genes *htrB* and *msbB* in *V. fischeri* ES114, an isolate from the *E. scolopes*
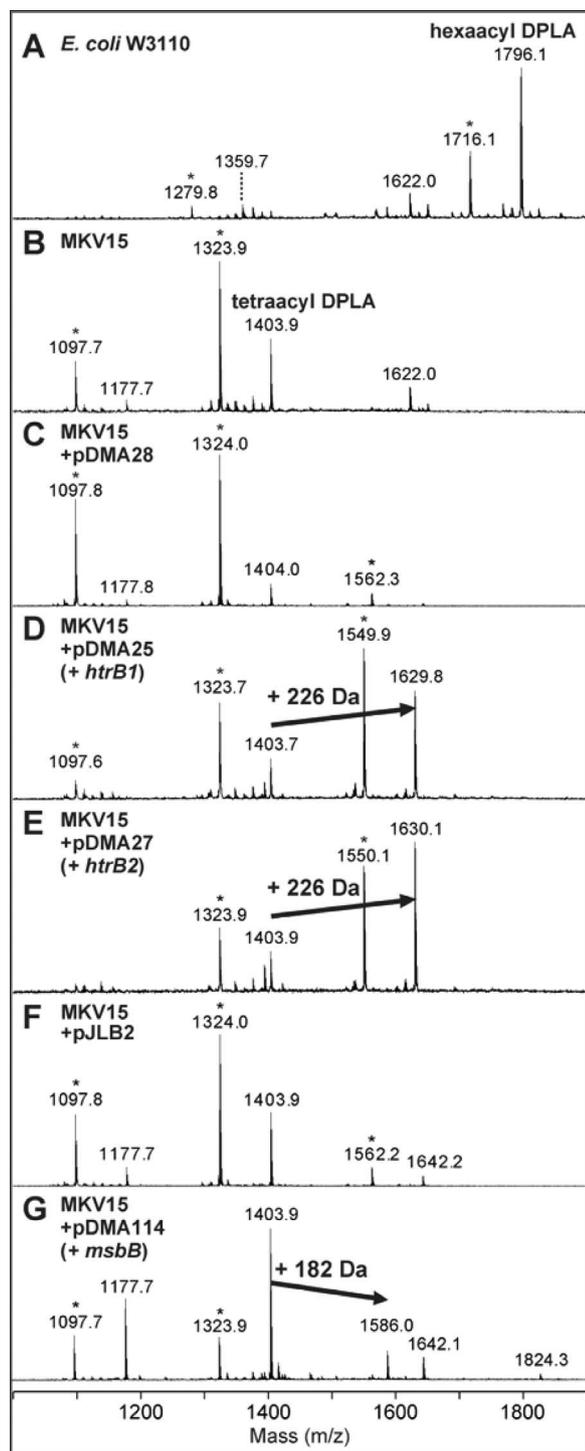
FIG. 2. Complementation of *E. coli* MKV15 with putative lipid A secondary acyltransferase genes from *V. fischeri*. Lipid A was obtained from LPS preparations of *E. coli* strains grown in minimal medium at 30°C, including W3110 (parent) (A), MKV15 (mutant lacking lipid A secondary acylations) (B), and MKV15 carrying plasmids with either no insert (pDMA28) [C] or pJLB2 [F]) or inserts of *htrB1*, *htrB2*, and *msbB* from *V. fischeri* (D, E, and G, respectively). pDMA28 served as the isogenic insert-free control for pDMA25 and pDMA27, whereas pJLB2 served this purpose for pDMA114. Samples were analyzed by negative-ion MALDI-TOF MS in the reflectron mode. The (M − H)$^-$ ion at *m/z* 1,796.1 (A) arises from *E. coli* DPLA. Strain MKV15 produces a tetra-acylated DPLA with an (M − H)$^-$ ion at *m/z* 1,403.9

light organ (1). Initially, we used PCR-based approaches with primers targeting conserved regions of these genes to identify two *htrB* homologs, designated *htrB1* and *htrB2*, and one *msbB* homolog, and to clone the full-length *htrB1* gene from an extant library. Subsequent sequencing of the ES114 genome (41) confirmed the presence of these genes and no other *htrB* or *msbB* homologs and enabled us to clone *htrB2* and *msbB*. The *V. fischeri* htrB1 (VFA0687), htrB2 (VF0122), and msbB (VF1799) genes encode proteins that are at least 36% identical and 53% similar to their respective homologs in *E. coli*. Interestingly, the two *V. fischeri* htrB genes are significantly diverged from each other, with only 48% and 53% identity in nucleotide and amino acid comparisons, respectively.

The genomic context of *htrB1*, *htrB2*, and *msbB* provided insight into their roles. Notably, the *htrB2* and *msbB* genes are located on the relatively large conserved vibrio "housekeeping" chromosome 1, whereas *htrB1* is on the more variable and species-specific chromosome 2 (Fig. 1). We also compared these genes to the putative lipid A secondary acyltransferase genes present in fully sequenced genomes of four other vibrios, namely, *Vibrio cholerae* O1 biovar Eltor strain N16961 (19), *Vibrio parahaemolyticus* RIMD 2210633 (29), *Vibrio vulnificus* CMCP6 (24), and *Vibrio vulnificus* YJ016 (5). As in *V. fischeri* ES114, each of these four vibrios has one *msbB* homologue located on chromosome 1. Each of these strains also has an *htrB* gene on chromosome 1 immediately downstream of a gene encoding a putative *tetR* family regulator, an organization conserved for *V. fischeri* htrB2 (Fig. 1). In addition to this conserved organization, the translated sequences of these four other *Vibrio htrB* genes are also the closest four matches to the *V. fischeri* HtrB2 sequence. Only *V. parahaemolyticus* RIMD2210633 has additional *htrB* genes (two of them), but neither shares the genetic context and localization to chromosome II of *V. fischeri* htrB1. These bioinformatic data suggest that *V. fischeri* htrB2 and *msbB* are evolutionarily conserved in the *Vibrionaceae*, whereas *htrB1* may perform a more niche-specific activity for *V. fischeri*.

Lipid A acyltransferase activity of *V. fischeri* htrB1, htrB2, and msbB. To test whether *V. fischeri* htrB1, htrB2, and msbB encoded lipid A acyltransferases, we placed these genes on plasmids in *E. coli* mutant MKV15 (*htrB*::Tn*10 msbB*::*cam lpxP*::*kan*), which lacks secondary acylations on lipid A (56). Lipid A samples were prepared from these and control strains by mild acid hydrolysis of the LPS, partially purified, and analyzed by MS. Figure 2 shows a stack plot of the MALDI spectra of these lipid A samples. The major lipid A components obtained from wild-type *E. coli* are a diphosphorylated lipid A (DPLA) and a monophosphorylated lipid A (MPLA), each containing four 3-hydroxymyristic acids (3-OH $C_{14:0}$), one myristic acid ($C_{14:0}$), and one lauric acid ($C_{12:0}$), yielding (M −

(B), which is also seen in MKV15 with the control plasmids (C and F). Arrows in panels D, E, and G indicate the molecular weight shifts caused by complementation. Peaks marked with asterisks are monophosphorylated lipid A forms. The small peak at *m/z* 1,622.0 (A and B) is an unidentified impurity. The minor addition of a $C_{16:0}$ fatty acid (238 Da) occasionally occurred even in the negative controls (C, F, and G).

TABLE 2. Percent fatty acid compositions of partially purified lipid A molecules from *V. fischeri* ES114 and mutant derivatives

Strain	% of indicated moiety										
	$C_{12:0}$	$C_{14:0}$	$C_{16:0}$	$C_{16:1}$ a	$C_{16:1}$ b	3-OH $C_{12:0}$	$C_{18:0}$	$C_{18:1}$ a	$C_{18:1}$ b	3-OH $C_{14:0}$	3-OH $C_{14:1}$
ES114 (wild type)	5.2	10.6	14.6	3.7	15.6	20.0	4.4	0.9	1.2	15.5	8.4
EVS300 (*htrB1*)	4.2	12.4	17.8	3.9	15.3	19.2	5.0	1.3	1.6	12.9	6.5
DMA310 (*htrB2*)	4.1	4.8	16.2	4.0	17.2	20.4	4.6	1.1	1.7	18.1	7.7
HG320 (*msbB*)	1.0	10.4	22.6	3.0	17.8	16.4	9.5	1.6	1.7	11.8	4.4
DMA330 (*htrB1 htrB2*)	1.3	4.4	19.9	3.2	21.5	20.6	7.2	0.8	3.3	11.3	6.5
DMA331 (*htrB1 msbB*)	0.8	11.4	21.2	3.5	17.1	16.2	8.9	1.7	1.5	12.1	5.5
DMA332 (*htrB2 msbB*)	1.0	5.2	20.1	2.5	18.8	16.8	7.5	1.4	1.8	18.9	6.0
AO340 (*htrB1 htrB2 msbB*)	0.9	6.0	17.5	4.2	24.8	17.6	8.8	1.5	2.3	10.8	5.6

H)⁻ ions for DPLA and MPLA at *m/z* 1,796.1 and 1,716.1, respectively. As previously reported (56), MKV15 lipid A lacks both of the secondary acyl chains ($C_{12:0}$ and $C_{14:0}$), yielding DPLA and MPLA with $(M - H)^-$ ions at *m/z* 1,403.9 and 1,323.9, respectively (Fig. 2). This was unaffected by either of the insertless plasmids, pDMA28 and pJLB2 (Fig. 2), although in some samples these negative controls contained small amounts of lipid A that were 238 Da larger, consistent with the addition of a $C_{16:0}$ moiety.

Each of the *V. fischeri htrB1*, *htrB2*, and *msbB* genes directed acylation of MKV15 lipid A, although their acyl chain substrates differed from those of their *E. coli* homologues. When MKV15 was transformed with plasmids carrying *V. fischeri htrB1* or *htrB2*, a 226-Da moiety was added to lipid A (Fig. 2), suggesting the addition of a hydroxylated $C_{14:0}$ fatty acid. This result suggests that *htrB1* and *htrB2* encode enzymes with a different substrate specificity from that of *E. coli* HtrB, which adds a lauric acid ($C_{12:0}$) to *E. coli* lipid A. Similarly, MKV15 complemented with *V. fischeri msbB* added a 182-Da moiety ($C_{12:0}$ fatty acid) to lipid A (Fig. 2), whereas *E. coli* MsbB adds a myristic acid ($C_{14:0}$). FAME analyses of lipid A molecules from the strains shown in Fig. 2 were consistent with our interpretation of these strains' lipid A mass profiles and confirmed that *V. fischeri msbB* directed the addition of $C_{12:0}$ to MKV15 lipid A, while *htrB1* and *htrB2* were responsible for the addition of 3-OH $C_{14:0}$ (data not shown). These results demonstrate that the *V. fischeri htrB1*, *htrB2*, and *msbB* gene products have lipid A acylase activity and suggest that their substrate specificities differ from those of their respective homologs in *E. coli*.

We further investigated the activities of *htrB1*, *htrB2*, and *msbB* by generating *V. fischeri* mutants lacking these genes and examining their lipid A molecules. FAME analyses of partially purified LPSs from ES114 and mutant strains are shown in Table 2. These data must be interpreted cautiously, because the structure of *V. fischeri* lipid A is unknown and appears to contain unusual modifications, but they are informative nonetheless. For example, each of the mutants lacking *msbB* had a reduced $C_{12:0}$ composition (Table 2), consistent with the apparent activity of *V. fischeri msbB* in transgenic *E. coli* (Fig. 2). Also, each of the mutants lacking *htrB2* had a reduction in $C_{14:0}$, although no difference in the 3-OH $C_{14:0}$ content was detectable. The *htrB1* mutant showed no clearly significant differences from the wild type, although strains lacking *htrB1* tended to have a relatively low 3-OH $C_{14:0}$ content. A more dramatic effect of *htrB1* was evident upon comparing the *htrB1*

htrB2 mutant to the *htrB2* mutant, which revealed a decrease in $C_{12:0}$ associated with the mutant *htrB1* allele (Table 2). This is consistent with other phenotypes measured in culture (reported below) in that effects of mutating *htrB1* were evident only in other mutant backgrounds. Taken together, these data further indicate that HtrB1, HtrB2, and MsbB direct the modification of lipid A in *V. fischeri*, although the activity of HtrB1 may be insignificant in the wild type grown in culture.

Sensitivity of mutants to SDS, kanamycin, and polymyxin B. Changes to the acylation pattern of lipid A can affect outer membrane stability and the resistance of bacteria to detergents, antibiotics, and host-derived antimicrobial peptides (17). Therefore, antimicrobial sensitivity assays provide a direct test of the barrier function of LPS and an indirect test for alterations in LPS structure. Notably, the activity of the antimicrobial peptide polymyxin B is thought to involve direct binding to lipid A, and alterations in lipid A structure can influence polymyxin B resistance. We determined the IC_{50}s of SDS, kanamycin, and polymyxin B for the wild-type strain ES114 and each of the *htrB1*, *htrB2*, and *msbB* mutants (Table 3). The *htrB1* mutant EVS300 was essentially like the wild type with respect to antimicrobial sensitivity. In contrast, *htrB2* mutant DMA310 and *msbB* mutant HG320 were each more sensitive to kanamycin and more resistant to polymyxin B, with DMA310 also displaying significantly increased sensitivity to SDS (Table 3). Combining mutations often resulted in more pronounced effects on antimicrobial sensitivity. Moreover, statistical analyses revealed significant allelic interactions leading to IC_{50}s that were not simply additive effects. This is illustrated by the influence of the presence or absence of *htrB2* on the effect that *htrB1* has on SDS sensitivity. Mutating *htrB1* in the wild-type background had little or no effect on growth in SDS, but in an *htrB2* mutant background, mutating *htrB1* caused a dramatic increase in SDS sensitivity. Thus, the data in Table 3 are consistent with *htrB2* and *msbB* affecting lipid A structure, whereas the effect of *htrB1* is negligible for the wild type growing in culture and is evident only in other mutant backgrounds.

Growth, luminescence, and motility of *V. fischeri* lipid A mutants in culture. One goal of this study was to examine the symbiotic competence of the *htrB1*, *htrB2*, and *msbB* mutants; however, we considered the possibility that these mutations might cause pleiotropic effects on cells, making it difficult to interpret whether any deficiencies in host colonization reflected symbiosis-specific defects. In particular, to fully colonize the *E. scolopes* light organ, *V. fischeri* must be able to swim (15), grow rapidly (40), and bioluminesce (54), and we there-

TABLE 3. Effects of *htrB* and *msbB* mutations on *V. fischeri* sensitivity to SDS, polymyxin B, and kanamycin

Strain	Genotype	$IC_{50}{}^{a}$		
		SDS (%)	Kanamycin ($\mu g\ ml^{-1}$)	Polymyxin B ($\mu g\ ml^{-1}$)
ES114	Wild type	10 (8.8–11)	104 (96–113)	0.73 (0.66–0.79)
EVS300	*htrB1::erm*	9.5 (8.3–10.7)	106 (98–115)	0.58 (0.54–0.62)
DMA310	Δ*htrB2::erm*	3.5 (3.2–4.0)*	74 (68–80)*	1.1 (1.0–1.2)*
HG320	Δ*msbB::erm*	7.1 (6.4–8.0)	66 (61–71)*	1.6 (1.4–1.8)*
DMA330	*htrB1::erm* Δ*htrB2*	0.031 (0.029–0.035)*	35 (32–38)*	1.7 (1.5–1.9)*
DMA331	*htrB1::erm* Δ*msbB*	7.0 (6.2–7.9)	59 (54–64)*	1.5 (1.3–1.6)*
DMA332	Δ*msbB::erm* Δ*htrB2*	2.0 (1.8–2.2)*	47 (44–51)*	4.7 (4.3–5.1)*
AO340	*htrB1::erm* Δ*htrB2* Δ*msbB*	0.024 (0.022–0.026)*	35 (32–38)*	2.6 (2.1–3.18)*

^{a} The IC_{50} is the concentration at which the growth yield is half-maximal (see Materials and Methods). Data represent combined results of three independent assays, and 95% confidence intervals are given in parentheses. Values marked with an asterisk indicate IC_{50}s that were significantly ($P < 0.01$) different from that of the wild type in each of the three independent assays.
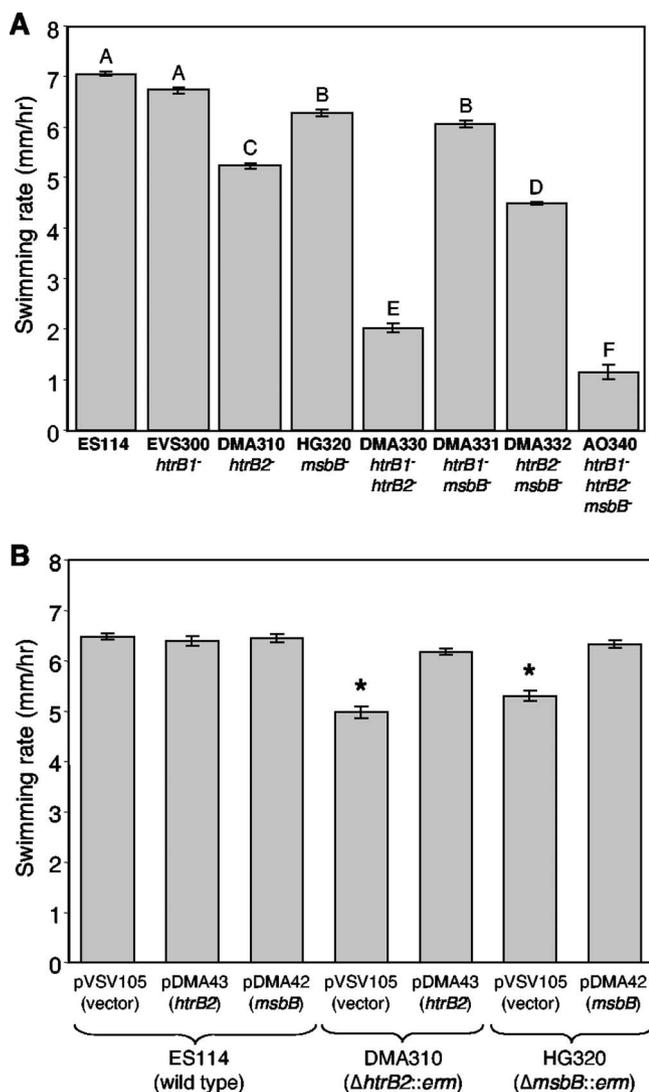

FIG. 3. Motility of *V. fischeri htrB1*, *htrB2*, and *msbB* mutants. Both panels report average rates of movement through 0.25% agar plates and show representative data from one of at least experiments. Standard errors ($n = 6$) are shown. (A) Motility of ES114 and mutants. Bars labeled with the same capital letter do not differ significantly ($P < 0.001$), as determined by ANOVA. (B) Motility of ES114, DMA310 (*htrB2*), and HG320 (*msbB*) with pVSV105, pDMA43 (pVSV105 + *htrB2*), or pDMA42 (pVSV105 + *msbB*). Asterisks represent significant differences ($P < 0.01$) from the wild type carrying the same vector.

fore examined these phenotypes in culture before examining the mutants' symbiotic competence.

We first assessed the ability of the *htrB1*, *htrB2*, and *msbB* mutants to swim through soft agar (Fig. 3A). The *htrB1* mutant EVS300 had no detectable difference in swimming rate relative to the wild-type parent, ES114. In contrast, DMA310 (*htrB2*) and HG320 (*msbB*) displayed significant ($P < 0.001$) attenuation of motility (Fig. 3A), and this could be complemented in *trans* by restoring the *htrB2* and *msbB* genes, respectively (Fig. 3B). Combining mutations in the same strain caused more severe attenuation in swimming, particularly for strains lacking *htrB2* (Fig. 3A). Microscopic observations provided a possible mechanistic explanation for these motility defects (Fig. 4). Unlike ES114 (Fig. 4A) and *htrB1* mutant EVS300 (not shown), mutants DMA310 (*htrB2*), DMA330 (*htrB1 htrB2*), and DMA332 (*htrB2 msbB*) formed chains of cells (Fig. 4B and C). These mutant cells appeared septated but still linked together (Fig. 4B). The nonmotile mutant AO340 (*htrB1 htrB2 msbB*) formed large groups of cells that adhered together, as well as unusually shaped, large, and possibly unseptated cells (Fig. 4D). *V. fischeri* normally swims using polar flagella, and it seems plausible that multiple cells linked end to end would not be as motile as free individual cells.

We next tested the growth rates of the *htrB1*, *htrB2*, and *msbB* mutants in broth cultures. EVS300 (*htrB1*), DMA310 (*htrB2*), HG320 (*msbB*), DMA331 (*htrB1 msbB*), and DMA332 (*htrB2 msbB*) had no discernible difference in growth rate relative to their wild-type parent, ES114. AO340 (*htrB1 htrB2 msbB*) and DMA330 (*htrB1 htrB2*) grew extremely poorly in LBS medium; however, the addition of 55 mM $MgCl_2$ and 8 mM $CaCl_2$ to LBS medium restored growth to both strains, indicating that divalent cations are important for growth when both *htrB1* and *htrB2* are absent (data not shown). In SWT medium, which contains divalent cations, AO340 (*htrB1 htrB2 msbB*) and DMA330 (*htrB1 htrB2*) grew at rates similar to that of the wild type; however, when the culture OD_{595} was ~0.5, AO340 cells clumped, and the growth rate could no longer be determined by measuring OD_{595} or by enumerating CFU.

We also assayed each mutant's bioluminescence. EVS300 (*htrB1*) and DMA310 (*htrB2*) displayed wild-type-like luminescence; however, we found that DMA330 (*htrB1 htrB2*) and AO340 (*htrB1 htrB2 msbB*) each had decreased luminescence compared to ES114 (Fig. 5). HG320 (*msbB*), DMA331 (*htrB1 msbB*), and DMA332 (*htrB2 msbB*) each displayed at least a
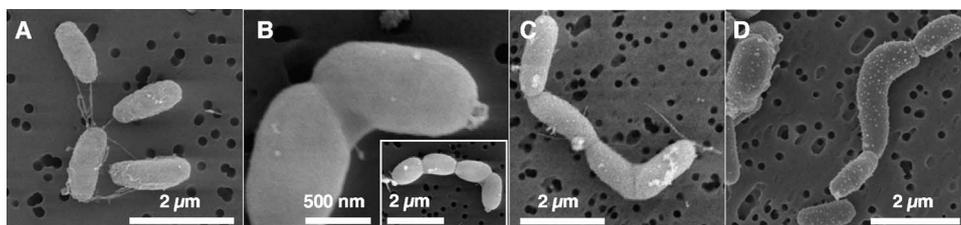
FIG. 4. Morphology of *htrB2* mutants. Scanning electron microscopy images of ES114 (wild type) (A), DMA310 (*htrB2*) (B), DMA330 (*htrB1 htrB2*) (C), and AO340 (*htrB1 htrB2 msbB*) (D) are shown.

twofold increase in specific luminescence relative to that of ES114 (Fig. 5), and this was complemented in HG320 by providing *msbB* in *trans* or by replacing the mutant deletion with the wild-type allele on the chromosome (data not shown). A potentially limiting substrate for the light-generating luciferase in *V. fischeri* is the aliphatic aldehyde that is (re)generated by LuxC and LuxE from the corresponding long-chain fatty acid, which is provided in part by LuxD (3, 44, 51). We speculated that eliminating MsbB might increase the substrate pool for luciferase, thereby resulting in the observed enhancement of luminescence. To test this, we added 10 μM myristic acid to the medium and found that the luminescence of both the wild type and HG320 (*msbB*) increased to the same level (data not shown), supporting the idea that MsbB and bioluminescence compete for a limited supply of long-chain fatty acids.

Taken together, the in-culture phenotypic characterization described above indicated that some, but not all, of the mutants were appropriate for symbiotic infection studies. EVS300 (*htrB1*) was indistinguishable from ES114 in culture, and therefore any attenuation during colonization of *E. scolopes* could be considered symbiosis specific, at least insofar as this mutant is not generally attenuated in growth. DMA310 (*htrB2*), HG320 (*msbB*), and DMA331 (*htrB1 msbB*) were also chosen

for symbiotic characterization, because their differences from the wild type were moderate. Other mutant strains were not included in symbiotic studies because of their low motility, decreased luminescence, odd cell morphology, and growth requirements.

Symbiotic colonization of *E. scolopes* by lipid A mutants. Despite their phenotypic differences from ES114 in culture (Tables 1 and 2; Fig. 3, 4, and 5), neither DMA310 (*htrB2*) nor HG320 (*msbB*) had an apparent defect in colonization of *E. scolopes* over 48 h following inoculation (data not shown). On the other hand, EVS300 (*htrB1*) and DMA331 (*htrB1 msbB*) appeared similarly attenuated relative to ES114 in the ability to initiate this symbiosis. For example, inoculation with EVS300 resulted in a reduced onset of symbiotic bioluminescence during initial colonization relative to that of animals inoculated with ES114 (Fig. 6A). This difference in symbiotic luminescence was subtle, and during initial colonization, ES114-infected animals became between 1.5- and 4-fold brighter than animals infected by EVS300. Moreover, this difference was reproduced in natural seawater, but in one experiment using Instant Ocean no difference was seen between the mutant and the wild type. Interestingly, we found that infections with the wild type or EVS300 were indistinguishable after the first light-triggered diurnal venting of symbionts (Fig. 6A).

Luminescence is a good indirect indicator of colonization levels in squid assays, and EVS300 produced luminescence indistinguishable from that of ES114 in culture (Fig. 5); however, we considered the possibility that differences in luminescence levels in EVS300- and ES114-infected animals did not reflect colonization levels. In a separate experiment, juvenile squid were infected with either ES114 or the *htrB1* mutant, and after luminescence of the two sets of animals diverged (Fig. 6B), we homogenized and plated the animals to determine CFU. EVS300-infected animals had fewer CFU than ES114-infected animals, confirming that less luminescence corresponded to fewer bacteria in the light organ in this experiment (Fig. 6C).

These experiments were technically challenging due to the light-triggered venting of the animals' symbionts and the lack of a discernible difference between animals infected with the wild type or *htrB1* mutants after the first venting. To obtain data like those in Fig. 6C, animal luminescence was monitored using a scintillation counter, and after the onset of luminescence, animals were plated while the room was kept as dark as possible to prevent triggering of the animals' venting behavior. We attempted to alleviate this problem by using competition experiments wherein animals were ex-
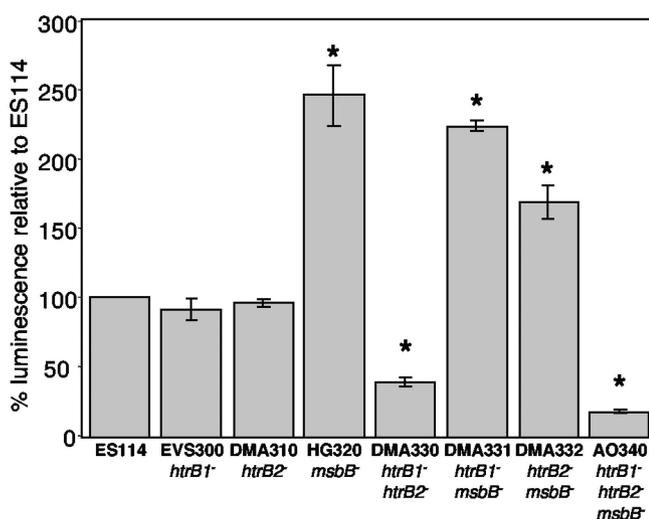

FIG. 5. Effects of *htrB1*, *htrB2*, and *msbB* mutations on biolumines-cence. The maximal luminescence per OD_{595} for mutant strains grown in SWT medium at 24°C is expressed as a percentage of that emitted by ES114. Error bars indicate standard errors ($n = 3$), and asterisks indicate significant differences from ES114 ($P < 0.05$). Data for one representative experiment of three are shown.
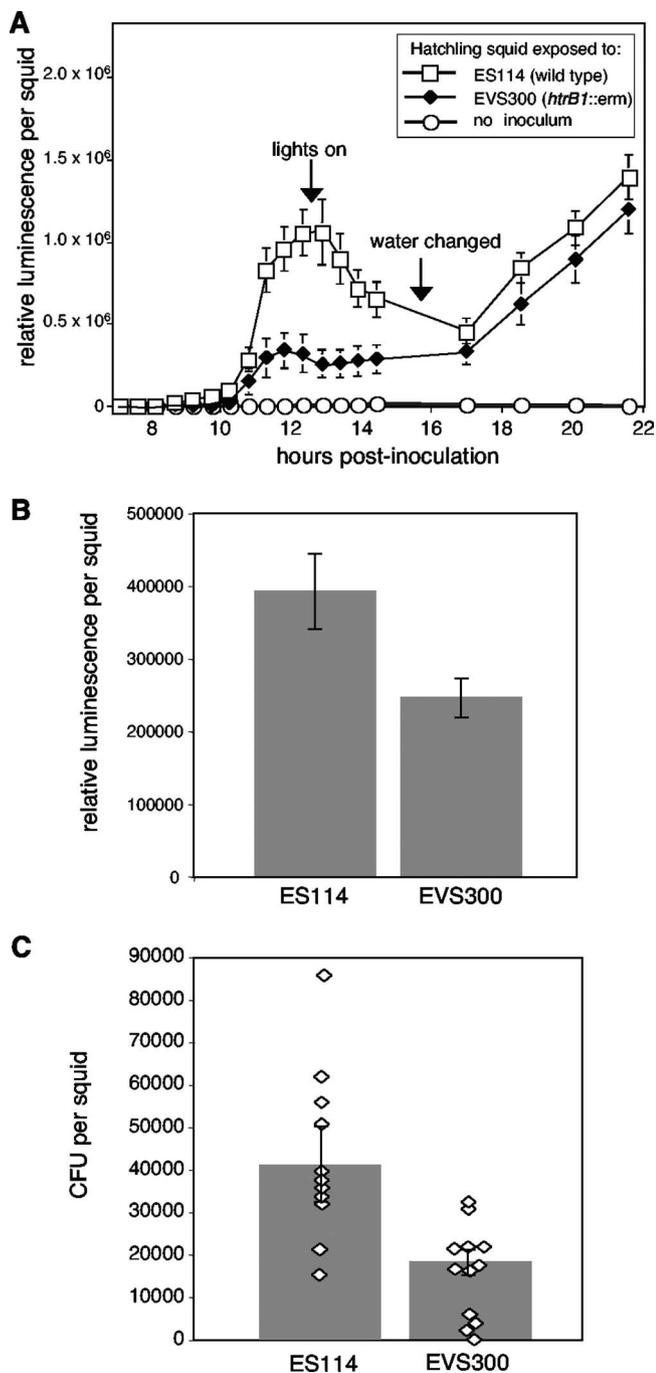
A

B

C

FIG. 6. Symbiotic luminescence and colonization of *V. fischeri* wild type and an *htrB1* mutant. (A) Animal luminescence during the initial stages of *E. scolopes* colonization by strains ES114 (wild type) and EVS300 (*htrB1* mutant). The luminescence pattern indicates the initial onset of colonization (0 to 12.5 h) followed by a changing level of light emission that reflects the diurnal venting behavior of the animal and regrowth of symbionts (2). Mean values for 21 animals were calculated, and standard errors of the means are indicated. (B) In a separate experiment, luminescence of hatchling squid inoculated with the wild type (ES114) or the *htrB* mutant (EVS300) was determined at 16 h postinoculation. Each bar represents the average for 11 or 12 animals, with the standard error. (C) Colonization levels of *V. fischeri* in the same animals as those presented in panel B. Each bar represents the average for 11 or 12 animals, with the standard error. Diamonds represent the CFU present in individual animals.
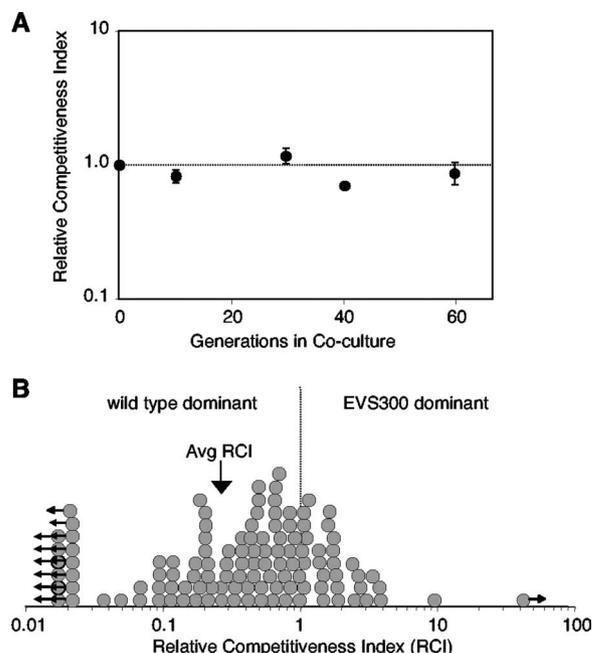
A

B

FIG. 7. Competition between ES114 and *htrB1* mutant EVS300 in culture and in squid. (A) Relative competitiveness of *htrB1* cocultured with ES114 in LBS medium. In parallel cultures, one strain or the other was tagged with *lacZ* to facilitate determination of strain ratios by blue-white screening (see Materials and Methods). Error bars represent standard errors ($n = 3$). (B) Relative competitiveness of *htrB1* mutant during colonization of *E. scolopes*. Juvenile squid were exposed to a mixed inoculum of the wild type and *htrB1* mutant EVS300 at a total concentration of ~2,500 CFU/ml, and the relative competitiveness was determined after 48 h. Circles represent the RCIs determined from infection of 118 individual animals. Circles with arrows represent animals that were clonally infected. Data represent combined results of four similar experiments.

posed to a 1:1 mixture of mutant and wild-type cells and the ratio of the two strains in the squid was determined at some time after infection. We reasoned that even if the mutant had a defect in only a narrow window of time during early infection, this might still be reflected in the populations later on, after venting. Another advantage of competition experiments is that variability between animals is less of a complicating factor because both strains are exposed to the same set of animals. Importantly, such competition experiments have been used in the past for studies of this symbiosis and have sometimes revealed colonization defects that are not immediately apparent in single-strain inoculations (27, 46, 55). To ensure that any competitive defect we might find would not simply reflect a generally attenuated mutant, we first competed ES114 and the *htrB1* mutant EVS300 in culture and found no competitive defect for the mutant under these conditions (Fig. 7A). However, when squid were co-inoculated with these strains, we found that the wild type outcompeted the *htrB1* mutant EVS300 by 2.7-fold (Fig. 7B). This is a similar magnitude of attenuation to that of the wild type that we saw during early infection in experiments with clonal inocula (Fig. 6A); however, these results were more reproducible and robust, and more animals could be analyzed because they did not have to be kept in the dark

and plated during a narrow window of time. In contrast to this competitive defect of the *htrB1* mutant, which was evident in the host and not in culture, the *msbB* mutant was not outcompeted by ES114 either in the symbiosis or in culture, and the *htrB2* mutant was outcompeted to a similar extent under both symbiotic and culture conditions (data not shown).

DISCUSSION

Despite intense interest regarding how lipid A structure affects pathogenic animal-bacterium interactions, little is known about how lipid A functions in a mutualism, such as the *V. fischeri*-*E. scolopes* symbiosis. *V. fischeri* is uniquely able to colonize and induce morphogenesis in the *E. scolopes* light organ, and previous evidence suggested that lipid A plays an important role in these processes (13, 25). In this study, we examined *htrB* and *msbB* genes, which encode lipid A secondary acyltransferases, to investigate their effects on the *V. fischeri*-*E. scolopes* mutualism and on the general biology of *V. fischeri*. Our results suggest that *htrB2* and *msbB* are conserved in other vibrios and that in *V. fischeri* they are active outside the symbiosis. This is illustrated by the observation that *htrB2* and *msbB* mutants displayed several phenotypic differences relative to the wild type in culture (Tables 2 and 3; Fig. 3, 4, and 5). In contrast, the *htrB1* gene, found on the more variable chromosome 2, appears distinctive of *V. fischeri*, and the *htrB1* mutant displayed a slight symbiosis-specific defect (Fig. 6 and 7) but was indistinguishable from the wild type in culture.

The symbiotic attenuation of the *htrB1* mutant was evident early in colonization (Fig. 6), possibly suggesting that HtrB1 modifies lipid A in a way that is important for symbiont recognition or other initial events in the infection. Indirect evidence for a role of lipid A and HtrB in signaling in this symbiosis came from Foster et al. (13), who found that LPS from a *Haemophilus influenzae htrB* mutant caused an attenuated apoptotic response in *E. scolopes* relative to that induced by LPS derived from wild-type *H. influenzae*. However, using a similar approach to that of Foster et al. (13), we did not detect a reduction in the apoptotic response in *E. scolopes* treated with LPS from the *V. fischeri htrB1* mutant relative to that after treatment with LPS from the wild-type strain (data not shown). If released LPS does act as a signal early in infection, one might expect that the wild type would compensate for the *htrB1* mutant when the strains are mixed; however, in mixed-strain competition experiments, the *htrB1* mutant was outcompeted by the wild type (Fig. 7). This may indicate that HtrB1 plays some role other than in signaling. On the other hand, significant segregation of strains occurs once cells colonize the light organ crypts during mixed infections (12), leaving open the possibility that a signaling defect of mutant cells in the crypt spaces cannot be compensated for by the wild type due to spatial separation. If so, it is possible that a signal conferred by HtrB1 is important in the early establishment of the symbiosis within the crypts rather than in the initial aggregation and migration of the bacteria on the surface of the light organ (34).

V. fischeri mutants lacking *htrB2*, *msbB*, or a combination of lipid A acyltransferase genes had unpredicted phenotypes, including motility defects, altered cell morphology, and enhanced bioluminescence (Fig. 3, 4, and 5). These observations

should be considered in examining the roles of *htrB* and *msbB* in host-bacterium interactions. Numerous studies in pathogenic organisms, including *Salmonella enterica* serovar Typhimurium and *E. coli*, show that *htrB* or *msbB* mutants colonize their animal hosts poorly or are less able to evade the immune system, suggesting a direct link between lipid A structure and virulence (22, 30, 42). However, motility contributes to colonization and virulence in these and other bacteria (26, 48), and motility was not reported in these studies of *msbB* and *htrB* mutants. We have now shown that *htrB2* and *msbB* mutants have attenuated motility, at least in *V. fischeri* (Fig. 3). Similarly, a recent study found that mutations in *htrB* or *msbB* in *E. coli* could have pleiotropic effects by affecting expression of the alternative sigma factor σ^E (50). Therefore, mutating *htrB* and *msbB* in pathogens could affect virulence indirectly in unexpected ways, and thorough analyses of *htrB* and *msbB* mutants in culture are important to determine whether decreased virulence reflects a general attenuation of the mutant, an indirect effect through another virulence determinant, or a defect specific to a direct role of LPS in the pathogen-host interaction.

The structure of *V. fischeri* lipid A has been difficult to solve and may include novel decorations. However, we have gained insight into the biochemical roles of *htrB1*, *htrB2*, and *msbB* by expressing these genes in an *E. coli* strain lacking secondary acylations on lipid A (Fig. 2) and by examining the fatty acid profiles of lipid A molecules from *V. fischeri* mutants (Table 2). Interestingly, both approaches indicated that *V. fischeri* MsbB adds a $C_{12:0}$ fatty acid to lipid A, in contrast to the $C_{14:0}$ acylation added by *E. coli* MsbB. This suggests that comparisons of *E. coli* and *V. fischeri* MsbB proteins could offer a powerful approach toward determining the acyl chain substrate specificities of MsbB enzymes. The $C_{12:0}$ content of lipid A was also decreased in an *htrB1 htrB2* double mutant (Table 2). Given the lack of evidence that either HtrB1 or HtrB2 uses $C_{12:0}$ as a substrate, these data could indicate that *V. fischeri* MsbB works most efficiently on lipid A that has already been decorated by the activity of HtrB, as is the case in *E. coli* (6, 7).

The direct activities of *V. fischeri* HtrB1 and HtrB2 are less clear, although they also seem to differ from their namesake in *E. coli*, which directs the addition of a $C_{12:0}$ moiety to lipid A. For example, the *V. fischeri htrB1* and *htrB2* genes each directed the addition of 3-OH $C_{14:0}$ to lipid A in transgenic *E. coli* (Fig. 2). Hydroxylated secondary acylations of lipid A are unusual but not unprecedented, and they have been observed on lipid A in *Bordetella hinzii* (2-OH $C_{14:0}$), *Bordetella trematum* (2-OH $C_{14:0}$), and *Rhizobium etli* (27-OH $C_{28:0}$) (4, 53). Consistent with the results for transgenic *E. coli*, *V. fischeri* strains lacking *htrB1* apparently tended to have a lower 3-OH $C_{14:0}$ content in their lipid A (Table 2), although this subtle trend in our data may not reflect a real effect. In contrast, there was no indication that *htrB2* mutants had decreased 3-OH $C_{14:0}$ in their lipid A. If anything, lipid A from *htrB2* mutant strains had slightly elevated levels of this fatty acid (Table 2). Instead, the *htrB2* mutant had a decrease in the $C_{14:0}$ component of lipid A (Table 2). This discrepancy between the apparent roles of *htrB2* in transgenic *E. coli* and *V. fischeri* could reflect different substrate structures and availability in these organisms. Ongoing attempts to elucidate the structure of *V. fischeri* LPS may help to resolve the activities of HtrB1 and HtrB2.

Future studies of lipid A and LPS in *V. fischeri* should consider the possibilities that factors other than lipid A are important in the signaling between *V. fischeri* and *E. scolopes* and that the signaling effects of lipid A may be codependent on other signaling molecules. Koropatnick et al. (25) found that *V. fischeri* releases peptidoglycan (PG) monomers that are structurally identical to those released by *Bordetella pertussis*, which kills ciliated tracheal cells, leading to the symptoms of whooping cough. In *V. fischeri*, released PG monomer triggers regression of *E. scolopes* ciliated appendages, and PG monomer acts synergistically in combination with LPS to stimulate morphogenesis similar to that seen in an infection with symbiotic *V. fischeri* (25). Given this relationship between LPS and the PG monomer, it would be interesting to place the lipid acyltransferase mutations described here in a *V. fischeri* strain that also has a reduction in release of the PG monomer and to assess signaling-related phenotypes such as apoptosis and morphogenesis as well as colonization. This multivariant approach may give more insight into the effects of the lipid A mutants on colonization when the PG monomer is not present and perhaps show a more dramatic symbiotic effect. As suggested before, it seems increasingly likely that signaling in this bacterium-animal mutualism will involve multiple signals and complex interactions, similar to the recognition of pathogens by animal hosts (13, 25, 30).

REFERENCES

1. **Boettcher, K. J., and E. G. Ruby.** 1990. Depressed light emission by symbiotic *Vibrio fischeri* of the sepiolid squid *Euprymna scolopes*. J. Bacteriol. **172:** 3701–3706.
2. **Boettcher, K. J., E. G. Ruby, and M. J. McFall-Ngai.** 1996. Bioluminescence in the symbiotic squid *Euprymna scolopes* is controlled by daily biological rhythm. J. Comp. Physiol. A **179:**65–73.
3. **Boylan, M., C. Miyamoto, L. Wall, A. Grahm, and E. Meighen.** 1989. Lux C, D, and E genes of the *Vibrio fischeri* luminescence operon code for the reductase, transferase, and synthetase enzymes involved in aldehyde biosyntheses. Photochem. Photobiol. **49:**681–688.
4. **Caroff, M., L. Aussel, H. Zarrouk, A. Martin, J. C. Richards, H. Therisod, M. B. Perry, and D. Karibian.** 2001. Structural variability and originality of the Bordetella endotoxins. J. Endotoxin Res. **7:**63–68.
5. **Chen, C. Y., K. M. Wu, Y. C. Chang, C. H. Chang, H. C. Tsai, T. L. Liao, Y. M. Liu, H. J. Chen, A. B. Shen, J. C. Li, T. L. Su, C. P. Shao, C. T. Lee, L. I. Hor, and S. F. Tsai.** 2003. Comparative genome analysis of *Vibrio vulnificus*, a marine pathogen. Genome Res. **13:**2577–2587.
6. **Clementz, T., J. J. Bednarski, and C. R. H. Raetz.** 1996. Function of the *htrB* high temperature requirement gene of *Escherichia coli* in the acylation of lipid A. J. Biol. Chem. **271:**12095–12102.
7. **Clementz, T., Z. Zhou, and C. R. H. Raetz.** 1997. Function of the *Escherichia coli msbB* gene, a multicopy suppressor of *htrB* knockouts, in the acylation of lipid A. J. Biol. Chem. **272:**10353–10360.
8. **Darveau, R. P.** 1998. Lipid A diversity and the innate host responses to bacterial infection. Curr. Opin. Microbiol. **1:**36–42.
9. **DeLoney-Marino, C. R., A. J. Wolfe, and K. L. Visick.** 2003. Chemoattraction of *Vibrio fischeri* to serine, nucleosides, and *N*-acetylneuraminic acid, a component of squid light-organ mucus. Appl. Environ. Microbiol. **69:**7527–7530.
10. **D'Hauteville, H., S. Khan, D. J. Maskell, A. Kussak, A. Weintraub, J. Mathison, R. J. Ulevitch, N. Wuscher, C. Parsot, and P. J. Sansonetti.** 2002. Two *msbB* genes encoding maximal acylation of lipid A are required for invasive *Shigella flexneri* to mediate inflammatory rupture and destruction of the intestinal epithelium. J. Immunol. **168:**5240–5251.
11. **Dunn, A. K., M. O. Martin, and E. V. Stabb.** 2005. Characterization of pES213, a small mobilizable plasmid from *Vibrio fischeri*. Plasmid **54:**114–134.
12. **Dunn, A. K., D. S. Millikan, D. M. Adin, J. L. Bose, and E. V. Stabb.** 2006. New *rfp*- and pES213-derived tools for analyzing symbiotic *Vibrio fischeri* reveal patterns of infection and *lux* expression in situ. Appl. Environ. Microbiol. **72:**802–810.
13. **Foster, J. S., M. A. Apicella, and M. J. McFall-Ngai.** 2000. *Vibrio fischeri* lipopolysaccharide induces developmental apoptosis, but not complete morphogenesis, of the *Euprymna scolopes* symbiotic light organ. Dev. Biol. **226:** 242–254.
14. **Goodson, M. S., M. Kojadinovic, J. V. Troll, T. E. Scheetz, T. L. Casavant, M. B. Soares, and M. J. McFall-Ngai.** 2005. Identifying components of the NF-κB pathway in the beneficial *Euprymna scolopes-Vibrio fischeri* light organ symbiosis. Appl. Environ. Microbiol. **71:**6934–6946.
15. **Graf, J., P. V. Dunlap, and E. G. Ruby.** 1994. Effect of transposon-induced motility mutations on colonization of the host light organ by *Vibrio fischeri*. J. Bacteriol. **176:**6986–6991.
16. **Gunn, J. S.** 2001. Bacterial modification of LPS and resistance to antimicrobial peptides. J. Endotoxin Res. **7:**57–62.
17. **Guo, L., K. B. Lim, C. M. Poduje, M. Daniel, J. S. Gunn, M. Hackett, and S. I. Miller.** 1998. Lipid A acylation and bacterial resistance against vertebrate antimicrobial peptides. Cell **95:**189–198.
18. **Hanahan, D.** 1983. Studies on transformation of *Escherichia coli* with plasmids. J. Mol. Biol. **166:**557–580.
19. **Heidelberg, J. F., J. A. Eisen, W. C. Nelson, R. A. Clayton, M. L. Gwinn, R. J. Dodson, D. H. Haft, E. K. Hickey, J. D. Peterson, L. Umayam, S. R. Gill, K. E. Nelson, T. D. Read, H. Tettelin, D. Richardson, M. D. Ermolaeva, J. Vamathevan, S. Bass, H. Qin, I. Dragoi, P. Sellers, L. McDonald, T. Utterback, R. D. Fleishmann, W. C. Nierman, O. White, S. L. Salzberg, H. O. Smith, R. R. Colwell, J. J. Mekalanos, J. C. Venter, and C. M. Fraser.** 2000. DNA sequence of both chromosomes of the cholera pathogen *Vibrio cholerae*. Nature **406:**477–483.
20. **Henneke, P., and D. T. Golenbock.** 2002. Innate immune recognition of lipopolysaccharide by endothelial cells. Crit. Care Med. **30:**207–213.
21. **Heumann, D., and T. Roger.** 2002. Initial responses to endotoxins and gram-negative bacteria. Clin. Chim. Acta **323:**59–72.
22. **Jones, B. D., W. A. Nichols, B. W. Gibson, M. G. Sunshine, and M. A. Apicella.** 1997. Study of the role of the *htrB* gene in *Salmonella typhimurium* virulence. Infect. Immun. **65:**4778–4783.
23. **Jones, B. W., and M. K. Nishiguchi.** 2004. Counterillumination in the Hawaiian bobtail squid, *Euprymna scolopes* Berry (Mollusca: Cephalopoda). Mar. Biol. **144:**1151–1155.
24. **Kim, Y. R., S. E. Lee, C. M. Kim, S. Y. Kim, E. K. Shin, D. H. Shin, S. S. Chung, H. E. Choy, A. Progulske-Fox, J. D. Hillman, M. Handfield, and J. H. Rhee.** 2003. Characterization and pathogenic significance of *Vibrio vulnificus* antigens preferentially expressed in septicemic patients. Infect. Immun. **71:** 5461–5471.
25. **Koropatnick, T. A., J. T. Engle, M. A. Apicella, E. V. Stabb, W. E. Goldman, and M. J. McFall-Ngai.** 2004. Microbial factor-mediated development in a host-bacterial mutualism. Science **306:**1186–1188.
26. **Lane, M. C., V. Lockatell, G. Monterosso, D. Lamphier, J. Weinert, J. R. Hebel, D. E. Johnson, and H. L. Mobley.** 2005. Role of motility in the colonization of uropathogenic *Escherichia coli* in the urinary tract. Infect. Immun. **73:**7644–7656.
27. **Lee, K.-H., and E. G. Ruby.** 1994. Competition between *Vibrio fischeri* strains during initiation and maintenance of a light organ symbiosis. J. Bacteriol. **176:**1985–1991.
28. **Lee, K.-H., and E. G. Ruby.** 1994. Effect of the squid host on the abundance and distribution of symbiotic *Vibrio fischeri* in nature. Appl. Environ. Microbiol. **60:**1565–1571.
29. **Makino, K., K. Oshima, K. Kurokawa, K. Yokoyama, T. Uda, K. Tagomori, Y. Iijima, M. Najima, M. Nakano, A. Yamashita, Y. Kubota, S. Kimura, T. Yasunaga, T. Honda, H. Shinagawa, M. Hattori, and T. Iida.** 2003. Genome sequence of *Vibrio parahaemolyticus*: a pathogenic mechanism distinct from that of *Vibrio cholerae*. Lancet **361:**743–749.
30. **McFall-Ngai, M. J.** 2002. Unseen forces: the influence of bacteria on animal development. Dev. Biol. **242:**1–14.
31. **Miller, J. H.** 1992. A short course in bacterial genetics. Cold Spring Harbor Laboratory Press, Cold Spring Harbor, NY.
32. **Montgomery, M. K., and M. McFall-Ngai.** 1994. Bacterial symbionts induce host organ morphogenesis during early postembryonic development of the squid *Euprymna scolopes*. Development **120:**1719–1729.
33. **Netea, M. G., M. van Deuren, B. J. Kullberg, J.-M. Cavaillon, and J. W. M. Van der Meer.** 2002. Does the shape of lipid A determine the interaction of LPS with Toll-like receptors? Trends Immunol. **23:**135–139.
34. **Nyholm, S. V., E. V. Stabb, E. G. Ruby, and M. J. McFall-Ngai.** 2000. Establishment of an animal-bacterial association: recruiting symbiotic vibrios from the environment. Proc. Natl. Acad. Sci. USA **97:**10231–10235.
35. **Parducz, B.** 1967. Ciliary movement and coordination in ciliates. Int. Rev. Cytol. **21:**91–128.
36. **Phillips, N. J., B. Schilling, M. K. McLendon, M. A. Apicella, and B. W.**

Gibson. 2004. Novel modification of lipid A of *Francisella tularensis*. Infect. Immun. **72:**5340–5348.

37. **Pinheiro, J. C., and D. M. Bates.** 2000. Mixed-effects models in S and S-PLUS. Springer, New York, NY.

38. **Post, D. M., N. J. Phillips, J. Q. Shao, D. D. Entz, B. W. Gibson, and M. A. Apicella.** 2002. Intracellular survival of *Neisseria gonorrhoeae* in male urethral epithelial cells: importance of a hexaacyl lipid A. Infect. Immun. **70:**909–920.

39. **Robey, M., W. O'Connell, and N. P. Cianciotto.** 2001. Identification of *Legionella pneumophila rcp*, a *pagP*-like gene that confers resistance to cationic antimicrobial peptides and promotes intracellular infection. Infect. Immun. **69:**4276–4286.

40. **Ruby, E. G., and L. M. Asato.** 1993. Growth and flagellation of *Vibrio fischeri* during initiation of the sepiolid squid light organ symbiosis. Arch. Microbiol. **159:**160–167.

41. **Ruby, E. G., M. Urbanowski, J. Campbell, A. Dunn, M. Faini, R. Gunsalus, P. Lostroh, C. Lupp, J. McCann, D. Millikan, A. Schaefer, E. Stabb, A. Stevens, K. Visick, C. Whistler, and E. P. Greenberg.** 2005. Complete genome sequence of *Vibrio fischeri*: a symbiotic bacterium with pathogenic congeners. Proc. Natl. Acad. Sci. USA **102:**3004–3009.

42. **Somerville, J. E., Jr., L. Cassiano, B. Bainbridge, M. D. Cunningham, and R. P. Darveau.** 1996. A novel *Escherichia coli* lipid A mutant that produces an anti-inflammatory lipopolysaccharide. J. Clin. Investig. **97:**359–365.

43. **Somerville, J. E., Jr., L. Cassiano, and R. P. Darveau.** 1999. *Escherichia coli msbB* gene as a virulence factor and a therapeutic target. Infect. Immun. **67:**6583–6590.

44. **Stabb, E. V., M. S. Butler, and D. M. Adin.** 2004. Correlation between osmolarity and luminescence of symbiotic *Vibrio fischeri* strain ES114. J. Bacteriol. **186:**2906–2908.

45. **Stabb, E. V., K. A. Reich, and E. G. Ruby.** 2001. *Vibrio fischeri* genes *hvnA* and *hvnB* encode secreted NAD$^+$-glycohydrolases. J. Bacteriol. **183:**309–317.

46. **Stabb, E. V., and E. G. Ruby.** 2003. Contribution of *pilA* to competitive colonization of the squid *Euprymna scolopes* by *Vibrio fischeri*. Appl. Environ. Microbiol. **69:**820–826.

47. **Stabb, E. V., and E. G. Ruby.** 2002. RP4-based plasmids for conjugation between *Escherichia coli* and members of the Vibrionaceae. Methods Enzymol. **358:**413–426.

48. **Stecher, B., S. Hapfelmeier, C. Muller, M. Kremer, T. Stallmach, and W. D. Hardt.** 2004. Flagella and chemotaxis are required for efficient induction of *Salmonella enterica* serovar Typhimurium colitis in streptomycin-pretreated mice. Infect. Immun. **72:**4138–4150.

49. **Swords, W. E., D. L. Chanc, L. A. Cohn, J. Shao, M. A. Apicella, and A. L. Smith.** 2002. Acylation of the lipooligosaccharide of *Haemophilus influenzae* and colonization: an *htrB* mutation diminishes the colonization of human airway epithelial cells. Infect. Immun. **70:**4661–4668.

50. **Tam, C., and D. Missiakas.** 2005. Changes in lipopolysaccharide structure induce the σ^E-dependent response of *Escherichia coli*. Mol. Microbiol. **55:**1403–1412.

51. **Ulitzur, S., and J. W. Hastings.** 1979. Evidence for tetradecanal as the natural aldehyde in bacterial bioluminescence. Proc. Natl. Acad. Sci. USA **76:**265–267.

52. **van der Ley, P., L. Steeghs, H. J. Hamstra, J. ten Hove, B. Zomer, and L. van Alphen.** 2001. Modification of lipid A biosynthesis in *Neisseria meningitidis lpxL* mutants: influence on lipopolysaccharide structure, toxicity, and adjuvant activity. Infect. Immun. **69:**5981–5990.

53. **Vedam, V., E. L. Kannenberg, J. G. Haynes, D. J. Sherrier, A. Datta, and R. W. Carlson.** 2003. A *Rhizobium leguminosarum acpXL* mutant produces lipopolysaccharide lacking 27-hydroxyoctacosanoic acid. J. Bacteriol. **185:**1841–1850.

54. **Visick, K. L., J. Foster, J. Doino, M. McFall-Ngai, and E. G. Ruby.** 2000. *Vibrio fischeri lux* genes play an important role in colonization and development of the host light organ. J. Bacteriol. **182:**4578–4586.

55. **Visick, K. L., and E. G. Ruby.** 1998. The periplasmic, group III catalase of *Vibrio fischeri* is required for normal symbiotic competence and is induced both by oxidative stress and by approach to stationary phase. J. Bacteriol. **180:**2087–2092.

56. **Vorachek-Warren, M. K., S. Ramirez, R. J. Cotter, and C. R. H. Raetz.** 2002. A triple mutant of *Escherichia coli* lacking secondary acyl chains on lipid A. J. Biol. Chem. **277:**14194–14205.

57. **Wolfe, A. J., and H. C. Berg.** 1989. Migration of bacteria in semisolid agar. Proc. Natl. Acad. Sci. USA **86:**6973–6977.